REVIEW

Strategies and Tools for Structure Determination of Natural Products Using Modern Methods of NMR Spectroscopy

by **Nadja Bross-Walch**[a]), **Till Kühn**[b]), **Detlef Moskau**[b]), and **Oliver Zerbe***[a])

[a]) Institute of Organic Chemistry, University of Zurich, Winterthurerstrasse 190, CH-8057 Zurich (phone: +41-1-6354263; fax: +41-1-6356833; e-mail: oliver.zerbe@oci.unizh.ch)
[b]) *Bruker Biospin*, Industriestrasse, CH-8137 Fällanden

Introduction. – Modern spectroscopic methods have largely revolutionized compound identification and tremendously accelerated the pace at which isolated compounds can be identified nowadays. It is hard to believe that 50 years ago compounds still required tedious decomposition into known fragments, or, alternatively, total chemical synthesis to corroborate the proposed structures. However, when compound quantities are very small, total chemical synthesis for independent structure elucidation is still being performed in important cases.

Following the discovery of the nuclear magnetic resonance (NMR) phenomenon by physicists, chemists quickly recognized its use for the identification of organic compounds, and NMR instruments entered the laboratories of chemists. The 'early' days of NMR were characterized by establishing empirical rules through which chemical-shift information was translated into covalent and stereochemical information. Inevitably, extraction of chemical shifts was hampered by the poor resolution of the low-field instruments in those days, which also contributed to problems associated with second-order effects.

Much progress in terms of sensitivity, leading to much smaller requirements of sample quantities, was made by the introduction of *Fourier*-transform (FT) NMR [1], allowing for more rapid acquisition of spectra, and by the construction of cryomagnets with higher fields. These techniques have essentially provided the technology to routineously record ^{13}C-NMR spectra, and ^{13}C chemical shifts proved to be of much use for structure identification. Another important contribution was the development of two-dimensional (2D) NMR spectroscopy in the laboratories of *Ernst* [2] in Zurich, and *Freeman* [3] in Cambridge. The 2D-NMR experiments yielded data containing information on *correlations* of nuclei *via* scalar or dipolar couplings; and, therefore, coupled partners need no longer be identified based on the extracted scalar couplings or irradiation experiments. Further technological developments resulting in more-stable NMR systems, such as the use of pulsed-field gradients and probeheads with superior sensitivity, nowadays allow chemists to record full sets of 2D data in less than an hour, provided that sensitivity is not limited by small sample quantities, which, however, is frequently the case when compounds have been isolated from natural sources.

This article is intended to describe strategies for NMR-based natural-product identification for researchers entering into this field. It will provide an overview on

typical features of natural-product compound classes and, additionally, summarize latest technological improvements. Due to the large number of natural compounds, this review is by no means complete, but intended to present a broad overview on the most-often encountered types of molecules, and should outline successful strategies to recognize, assign, and identify them. It will suggest different strategies for structure identification and briefly describe experiments most useful for that task. The review is also far from being comprehensive with respect to what type of NMR experiments have been selected. We have limited the description of experiments on purpose to a minimal number, which will be sufficient in most of the cases. Nevertheless, the reader should be aware that alternatives or variants of the experiment exists that may be advantageous in particular cases. We have also limited our description to the most-common approaches in order to help newcomers to enter this field. Numerous reviews in the field of natural-product identification by NMR methods have been published [4] and the more-interested reader is referred to these sources. References to more specific papers have been provided in the appropriate corresponding subsections of this review. Readers more-interested in the technical details of how to perform NMR experiments in the best way may find some help in the recent review by *Reynolds* and *Enriquez* [5].

Although NMR data are probably the most-useful source of information for establishing molecular structures, they need to be complemented by other methods. This means, in particular, that no structure should be published that is not compatible with mass-spectral data! Last but not least we would like to remark that structure elucidation of natural products should always go hand in hand with a careful determination of biological activity, if not established yet, which usually comprises presentation of data on cytotoxicity or antibacterial potency.

The strategies proposed have been developed in courses taught to diploma and Ph.D. students majoring in chemistry, biochemistry, molecular biology, or pharmaceutical sciences. We have deposited much more elaborate material containing training sets of 2D spectra, shift tables, and other useful information on the internet, and we encourage the reader to download the corresponding material (see www.oci.unizh.ch/group.pages/zerbe/Course.html).

Technological Improvements. – While modifications in magnet technology or electronics have led to smooth, but steady, improvements over the years, the introduction of cryogenically cooled probe-heads [6][7] or the application of pulse-field gradients [8] have resulted in more-dramatic changes. The basic concept behind cryogenically cooled probes (so-called 'cryoprobes') is that, upon cooling the radio-frequency (RF) coil to a temperature of *ca.* 20 K, thermal noise is dramatically lowered, resulting in signal-to-noise (S/N) figures generally three to four times higher than for conventional probe heads. Considering that measuring time needs to be four times as long in order to improve the S/N by a factor of two, this effectively means that measurements that take a week on a normal probe can be done in less than a day, yielding similar spectra. Alternatively, much smaller sample quantities can be used, obviously a considerable advantage when working with compounds isolated from natural sources. It should be added here that cryoprobes require a complex cooling system including compressors, heat exchangers, *etc.*, and the total costs add up to an amount that would allow purchasing a low-field spectrometer itself. Still, we think that

the additional investments are well justified by the enormous increase in sensitivity. Obviously, experiments that involve less-sensitive or -abundant nuclei (such as ^{13}C) benefit a lot from such a gain in sensitivity, with the most-prominent example probably being the INADEQUATE technique [9].

Fig. 1,a displays data recorded with 150 μg of taxol using either a 5-mm cryoprobe (*ca.* 1 mM) or a 1-mm *MicroProbe* (total volume: 5 μl, concentration: *ca.* 40 mM). The $^{13}C\{1H\}$, the DEPT-135, and the HSQC spectra on the cryoprobe were recorded in 7 h 12 min, 3 h 40 min, or 1 h 50 min, respectively, on a *Bruker DCH CryoProbe* at 100/400 MHz, a field typically used for natural products. The latter probe has high sensitivity on both the carbon and the proton nuclei. Cryogenically cooled probes allow one to record ^{13}C-detected spectra at concentrations as low as 0.1 mM. The typical acquisition time for an INADEQUATE experiment with 25 mmol of compound, *e.g.*, 10 mg of quinine, with a *DCH CryoProbe* at 500 MHz, is only 15 h.

Since sensitivity is often mass-limited, 1- or 3-mm probe-heads or small rotors in combination with a magic-angle spinning (MAS) unit have been developed to allow the measurement of much smaller sample quantities. The 1-mm *MicroProbe* has a conventional RF coil at room temperature. *Fig. 1,b* presents HSQC and HMBC data of 150 μg of taxol, measured in 50 minutes or 12 h, respectively, using a 1-mm *MicroProbe* at 100/400 MHz. The spectra clearly demonstrate that, for mass-limited samples, a 1-mm *MicroProbe* presents a very attractive alternative to cryoprobes, provided that sample aggregation and solubility do not present a problem at such high concentrations.

Sensitivity itself is not the only determinant for spectral quality, the level of noise being another very important factor. Traditionally, selection of correct coherence-transfer pathways was performed using the concept of phase cycling and, therefore, relied on an addition/subtraction procedure. Any instability of the NMR system, mainly manifested as fluctuations of the field-frequency-regulation circuit (the 'lock') and often arising from fluctuations in room temperature or magnetic disturbances, may introduce such noise, which, in the worst case, may completely cover weak signals (for a more detailed discussion, see [10]). In experiments utilizing so-called pulsed-field gradients (PFGs), only the desired coherences enter into the receiver, and the effects from short-term fluctuations are much less disastrous. Noise in heteronuclear experiments such as long-range H,C correlations [11] is enormously reduced in experiments with PFGs. It should be noted here that the use of PFGs is usually accompanied by a loss in sensitivity by a factor of $1/\sqrt{2}$, and in the case of very small sample quantities, HSQC experiments with conventional phase cycling may yield superior spectra.

Another development important for the analysis of natural products are 'hyphenated' techniques such as liquid-chromatography (LC) NMR. NMR has always been a preferred method for structural elucidation of natural products or compounds that have to be purified by HPLC in the final step. There are several methods to deliver the HPLC fraction to the NMR coil, as depicted in *Fig. 2*. Many of them involve flow NMR methods, where the HPLC fraction is transferred *via* capillaries into a flow NMR probe. Most techniques involve a large degree of automation and can be run nonsupervised using a previously optimized LC method. Here, we describe the most frequently used methods to transfer LC fractions into an NMR instrument.

The simplest way is to couple the HPLC directly to the NMR spectrometer, and to perform an on-flow analysis of the chromatographic fractions [12]. The drawback of

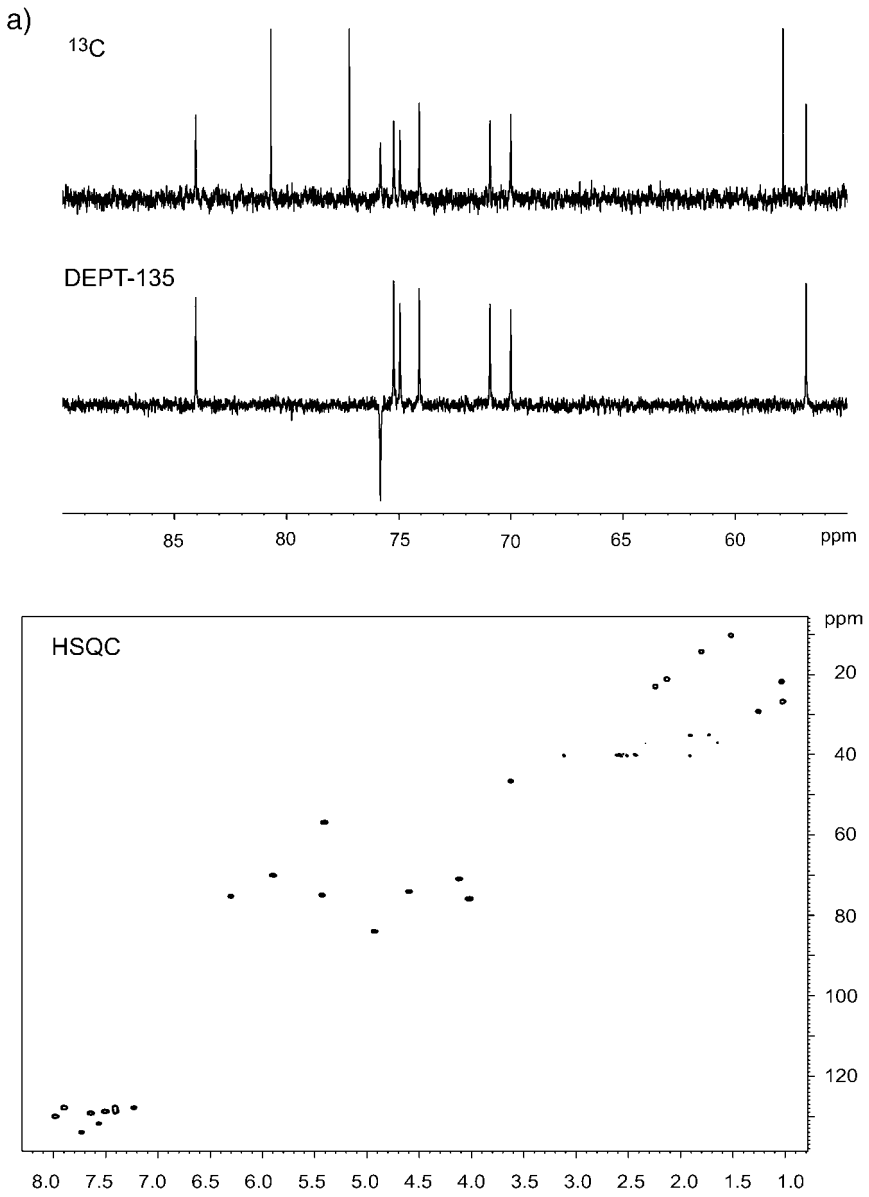

Fig. 1. *Different NMR spectra of taxol* (150 µg) *in (D$_6$)DMSO* (0.25 ml) *as a function of probe head. a*) *DCH CryoProbe,* 5-mm *Shigemi* NMR tube. *Top:* Expansions of the 100-MHz ^{13}C-NMR (upper part) and DEPT-135 (lower part) spectra. The acquisition times were 3 h 40 min and 7 h 12 min for the DEPT-135 and the ^{13}C-NMR spectra, resp. *Bottom:* 100/400-MHz [^{13}C,^{1}H]-HSQC spectrum after 1 h 50 min. *b*) *MicroProbe* (1 mm); *top:* HSQC spectrum after 50 min; *bottom:* HMBC spectrum after 12 h.

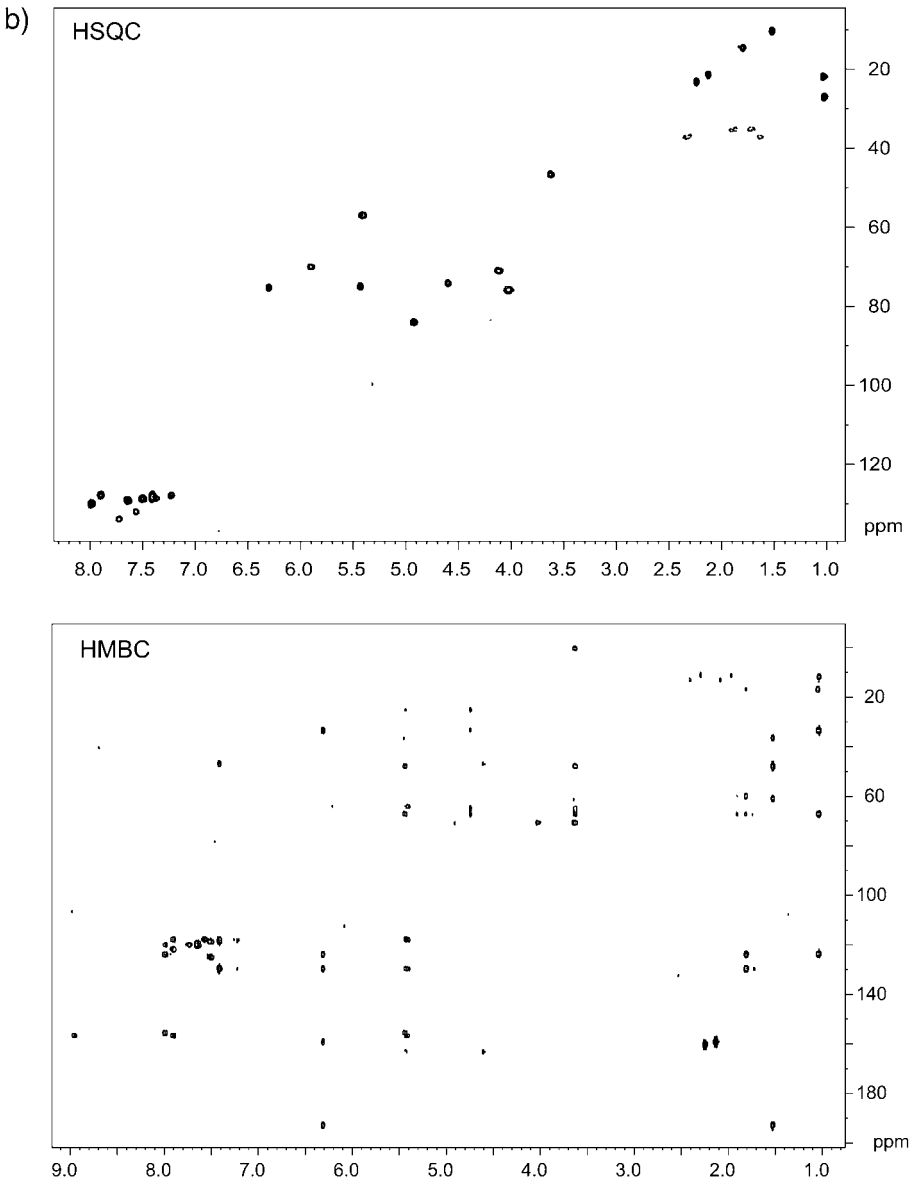

Fig. 1 (cont.)

this 'on-flow NMR' method is that the residence time of the sample in the NMR flow cell is determined by the flow supplied by the HPLC pump, and not by the time necessary to obtain a sufficient S/N ratio in the NMR spectrum. Therefore, this method only works well if the sensitivity is sufficient to obtain a spectrum in a few scans.

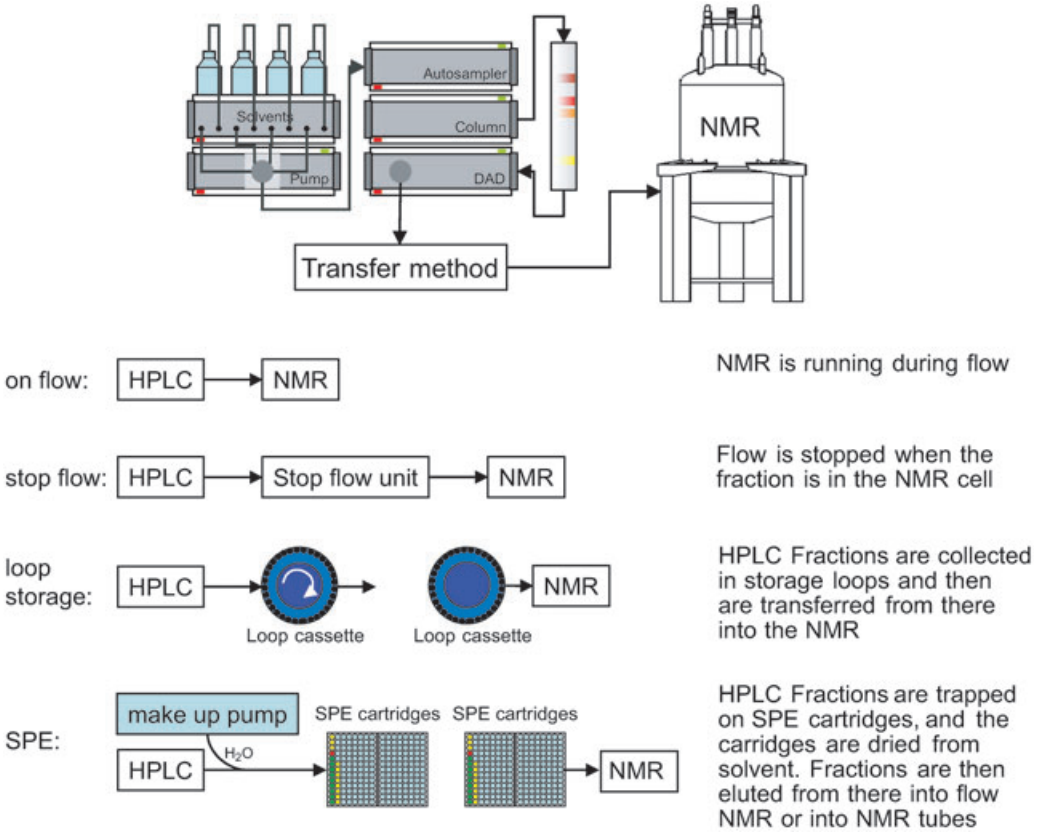

Fig. 2. *Various LC–NMR-coupled techniques* (see text)

The 'stopped-flow NMR' technique addresses this problem by stopping the flow of the HPLC pump as soon as a fraction of interest is inside the NMR flow cell, while keeping the LC pressure constant in order not to disturb the separation [13]. As soon as the NMR measurement of a given fraction is complete, chromatography is resumed under normal flow. This method may also be used for fractions with very low concentrations, but it proved to be more practical in many cases to collect the fractions in capillary storage loops during the nonstop HPLC elution, and to transfer these stored fractions into the NMR system independently from the ongoing separation [14]. This system is often referred to as 'loop storage' and has many advantages over the previous methods: the fractions can be measured in the NMR system as long as necessary, the chromatographic run is not disturbed, and the analysis runs in full automation with loop storage cassettes for independent fractions. An alternative to this technique is the so-called 'solid phase extraction' (SPE), where the HPLC fractions are collected on SPE cartridges [15]. These cartridges are very short chromatographic columns, which can be filled with different stationary phases. Typically, the flow in organic solvents (*e.g.*, MeCN) eluting from the HPLC is mixed with additional H_2O and, as a consequence of

the change in solvent polarity, trapped on an SPE cartridge. The fraction is eluted from the dried-out cartridge at an appropriate time either into an NMR flow probe or into an NMR tube by using an organic phase such as pure MeCN in a fully-automated fashion. The SPE technique has several advantages: the purified HPLC fractions typically elute in very small solvent volumes and are, thus, highly concentrated. Moreover, the whole chromatography can be run with regular protic solvents, and deuterated solvent is only required for elution from the dried cartridge. The HPLC fractions can be eluted from the SPE cartridges into a cryoprobe equipped with a flow accessory, or into 1-mm *MicroProbes* for best sensitivity performance.

A Set of Experiments. – The set of experiments and the strategy used for assignment and full structure elucidation very much depends on the compound to be identified. Smaller molecules, for which resonance overlap is not too serious and in which proton density is high, can be fully assigned based on homonuclear H,H shift-correlation experiments such as COSY [16], TOCSY [17][18], and ROESY [19][20] or NOESY [21] (see the *Appendix*). The spectra from double-quantum-filtered COSY (DQF-COSY) experiments contain cross-peaks due to vicinal and geminal couplings. The TOCSY spectra additionally contain correlations with other H-atoms *in the same spin system*, provided the mixing time has been chosen sufficiently long (usually 80–100 ms). TOCSY Spectra are extremely useful for compounds containing many separate spin systems *e.g.*, amino acid residues in peptides or monosaccharide units in carbohydrates. Provided the spin systems contain one resolved resonance, members of the same spin system can be easily identified. This technique, developed for oligosaccharides by *Vliegenthart et al.* [22], has become known as the *reporter-group concept*. For peptides, these nonoverlapping resonances are mainly the amide H-atoms, whereas for carbohydrates the anomeric region displays the best signal dispersion.

The classical experiment for obtaining stereochemical information but also for linking separate spin systems is NOESY. The magnitude of the nuclear *Overhauser* effect (NOE) between two H-atoms depends on the separating distance to the inverse sixth power, but also on motional properties of the molecule [23]. Even for very short distances, the NOE for molecules in a certain size range may actually be zero. The rotating-frame analog of NOESY, *i.e.*, ROESY, offers a very attractive alternative for smaller molecules, because the ROE is always positive. In addition, in a ROESY experiment, almost all kinds of possible artifacts such as exchange peaks, spin diffusion, or TOCSY transfer peaks, display a sign opposite to that of genuine ROEs and can, therefore, be easily distinguished. The T-ROESY experiment from *Shaka* and co-workers is a useful alternative to ROESY, in which the TOCSY transfer peaks are eliminated at the expense of somewhat reduced sensitivity [24].

Although TOCSY experiments help to reduce the problems associated with resonance overlap, all H,H correlation experiments suffer from the usually low resolution of ^{1}H-NMR spectra. Spin-system assignments in steroids clearly demonstrate how difficult it can be to walk through the spin-systems when signal overlap is serious. Moreover, cross-peaks of resonances with similar chemical shifts lie close to the diagonal and are, therefore, often difficult to recognize. In addition, small couplings, possibly in combination with broader lines, as encountered for larger molecules or in exchanging systems, lead to low efficiency for coherence transfer. An example is the

spin-system assignment in furanose *vs.* pyranose units of carbohydrates. The rigid, chair-like conformation in the latter in combination with large couplings for diaxial H-atoms leads to COSY spectra with good cross-peak intensities. In contrast, the situation encountered in the five-membered furanose rings is usually less favorable. To conclude, strategies exclusively relying on H,H correlation spectra are limited to small molecules with sufficient functionality so that resonance overlap is small or to larger but higher functionalized molecules with better chemical-shift dispersion such as peptides or (to a much smaller extent) oligosaccharides.

Obviously, the solution to many of the problems described in the previous two paragraphs is the use of spectra with carbon editing. In this context, the introduction of heteronuclear-correlation experiments with both proton excitation and proton detection (double-polarization-transfer experiments like HSQC [25], HMQC [26][27], or HMBC [28]) has dramatically reduced the required sample quantities, so that these spectra can be recorded with milligram or sub-milligram quantities on 1-mm *MicroProbes*. Moreover, PFG versions almost perfectly suppress residual signals from H-atoms bound to ^{13}C, resulting in high-quality spectra. An obvious advantage is that ^{13}C-NMR chemical shifts become accessible and, hence, databases may be used to more easily construct molecules [29][30]. Moreover, geminal H-atoms are immediately identified, which helps one to distinguish geminal from vicinal correlations in the COSY spectra.

A very useful alternative to the DQF-COSY experiments in case of small signal dispersion is HSQC-TOCSY [31]. In this hyphenated experiment, additional correlations due to the scalar H,H couplings are found. The good resolution along the C dimension allows one to easily recognize the coupled partners, provided the chemical-shift difference is larger than the width (in the H dimension) of the signal. An example for the use of such spectra is demonstrated for a steroid in *Fig. 3*. Therein, the correlation between H–C(6) and H–C(15)[1]) is difficult to establish in the DQF-COSY experiment due to the small chemical-shift separation of the signals, which results in cross-peaks being very close to the diagonal. In contrast, the correlation is clearly visible in the HSQC-TOCSY, and the strongly improved resolution is of great advantage, and often compensates for the reduced sensitivity of the experiment.

The linkage of spin systems was originally achieved *via* NOEs. With the advent of sensitive experiments for detecting H,C long-range interactions, especially the HMBC technique [28], this could also be achieved with the latter, and often both ways are used in a complementary fashion. Thereby, linkage points in carbohydrates are defined by using either NOEs between the H-atoms attached to the C-atoms involved in forming the glycosidic bond, or by using the corresponding three-bond H,C couplings. HMBC Experiments are especially important when the proton density is low so that ^{1}H-NMR spectra mainly contain *singlet* signals. A good example are flavonoids, for which the aromatic rings are often substituted to an extent that no scalar couplings and only few NOEs are observed.

In the ultimate case, compounds that contain no or very little H-atoms cannot be assigned or identified with the strategies depicted above. For such compounds, the

---

[1]) Please note that our atom numbering does not correspond to that normally used for steroids, but is based on the ^{13}C-NMR chemical-shifts.

skeleton needs to be mapped through the carbon 'backbone', and the famous INADEQUATE technique [9] is often the only possibility for spectral assignments. Unfortunately, sample-quantity requirements are often prohibitively high, although the introduction of cryoprobes has lowered requirements significantly. Moreover, 1- to 3-mm probe heads may also result in less-demanding sample-quantity restrictions, but 1-mm *MicroProbes* presently available are limited to H-atom detection. It is crucial to add some relaxation-promoting reagent (such as $Cr(Acac)_3$) to get *T1* values down into the 1-s range to allow for more-rapid pulsing. It is common experience in INADEQUATE spectra recorded with natural products that many correlations are missing. In this respect, it is very important to recognize that these spectra contain redundant information. The frequency displayed in the indirect dimension is the double-quantum frequency, which is the sum of the frequencies of the coupled partners. Correlations occur as peak *pairs* on a horizontal line, and when only a single peak is visible, the position of the second peak can be calculated simply by forming the difference of the double-quantum frequency to the position of the first peak. Still, quantities of isolated natural products will, unfortunately, often not allow recording these very useful spectra. For sensitivity reasons, the INADEQUATE experiment has often been replaced by its proton-detected version, the ADEQUATE technique [32]. However, the disadvantage of ADEQUATE is that correlations to quaternary C-atoms are lost, and often low proton density is just the reason why one would like to use INADEQUATE spectra.

Introduction of isotopic labels into molecules such as peptides or nucleic acids has stimulated the development of a plethora of triple-resonance experiments (for a review, see [33]), in which coherence is transferred in a predictable manner along the large one-bond couplings. However, these experiments would require feeding plants or organisms with enriched media. This has been done, *e.g.*, to produce ^{13}C-enriched silk for solid-state NMR, but these experiments will not be covered in this review.

For a schematic overview of the experiments described, see the *Appendix*. For a more-detailed description, see the excellent review by *Griesinger* and co-workers [34], which provides also a more-rigorous (but still well-understandable) description of the theory, or the books by *Freeman* [35], *Homans* [36], *Martin* and *Zektzer* [37], or *Croasmun* and *Carlson* [38].

Determination of Configuration. – Once the covalent structure of a molecule has been established, NOEs or ROEs are used to determine its configuration[2]). This is probably the most-difficult part during the NMR analysis, and is certainly more prone to errors when compared to crystallography. Wrong stereochemical assignments can be found in the literature because no 3D models have been used to estimate distances and compare it to observed NOEs. Many molecules, especially polycyclic systems, look quite different in three dimensions than on paper. Even if the model is crude and distances have large uncertainties, this is certainly preferable to the use of distances estimated from a simple sketch of the molecule. NOEs between vicinal H-atoms should only be used very carefully for establishing their relative configuration. Usually, this

---

[2]) A more elaborate account on the theory of NOE is beyond the scope of this review, and the interested reader is referred to the book of *Neuhaus* and *Williamson* [23].

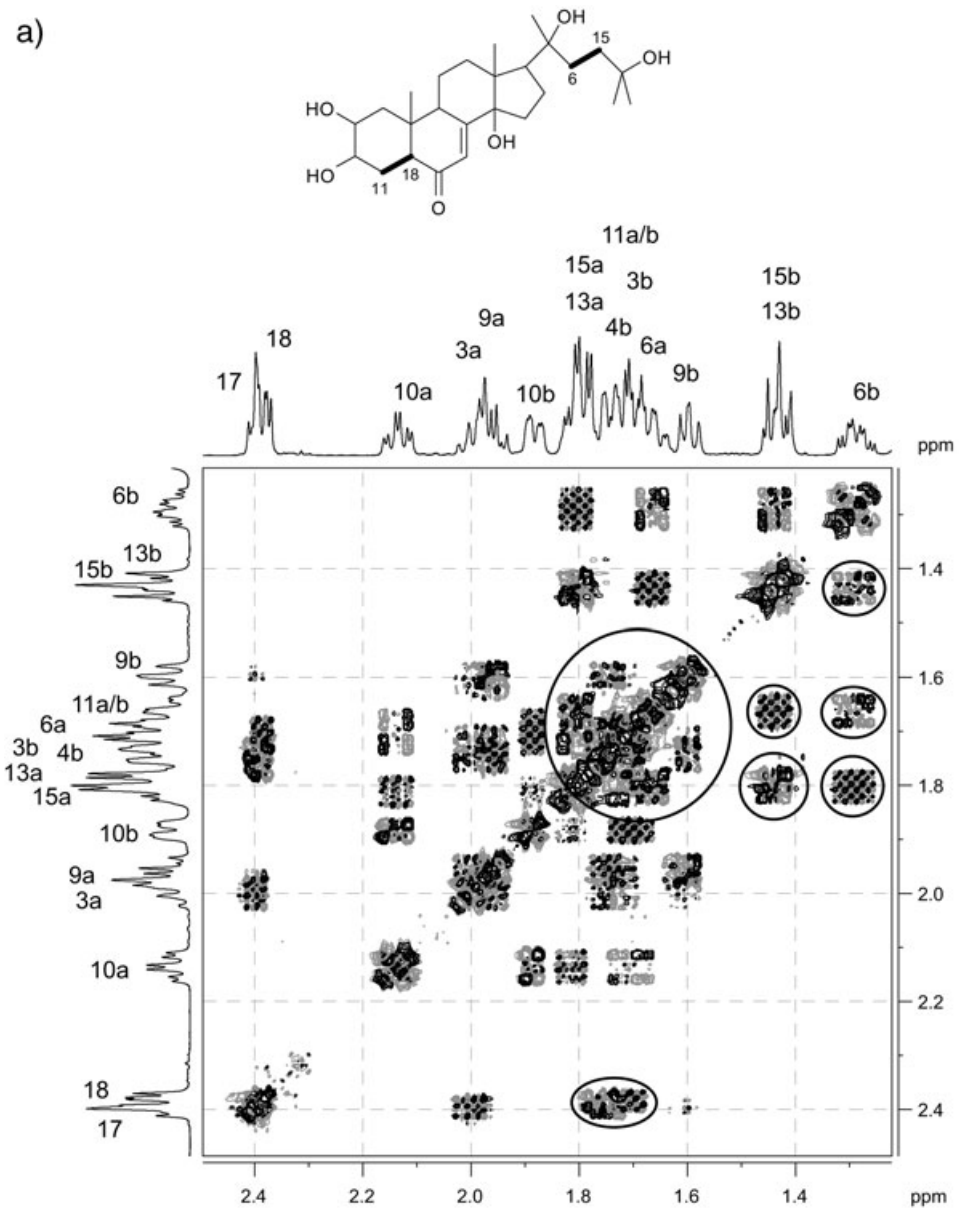

Fig. 3. *NMR Analysis of the steroid β-ecdyson*. Expansions of *a*) the DQF-COSY and *b*) the corresponding 12-ms HSQC-TOCSY spectra. Correlations from two fragments, printed in bold in the chemical drawing, are indicated in the spectra. Encircled signals are HSQC peaks. Note that numbering was made according to the ^{13}C-NMR spectrum and does not correspond to classical steroid numbering.

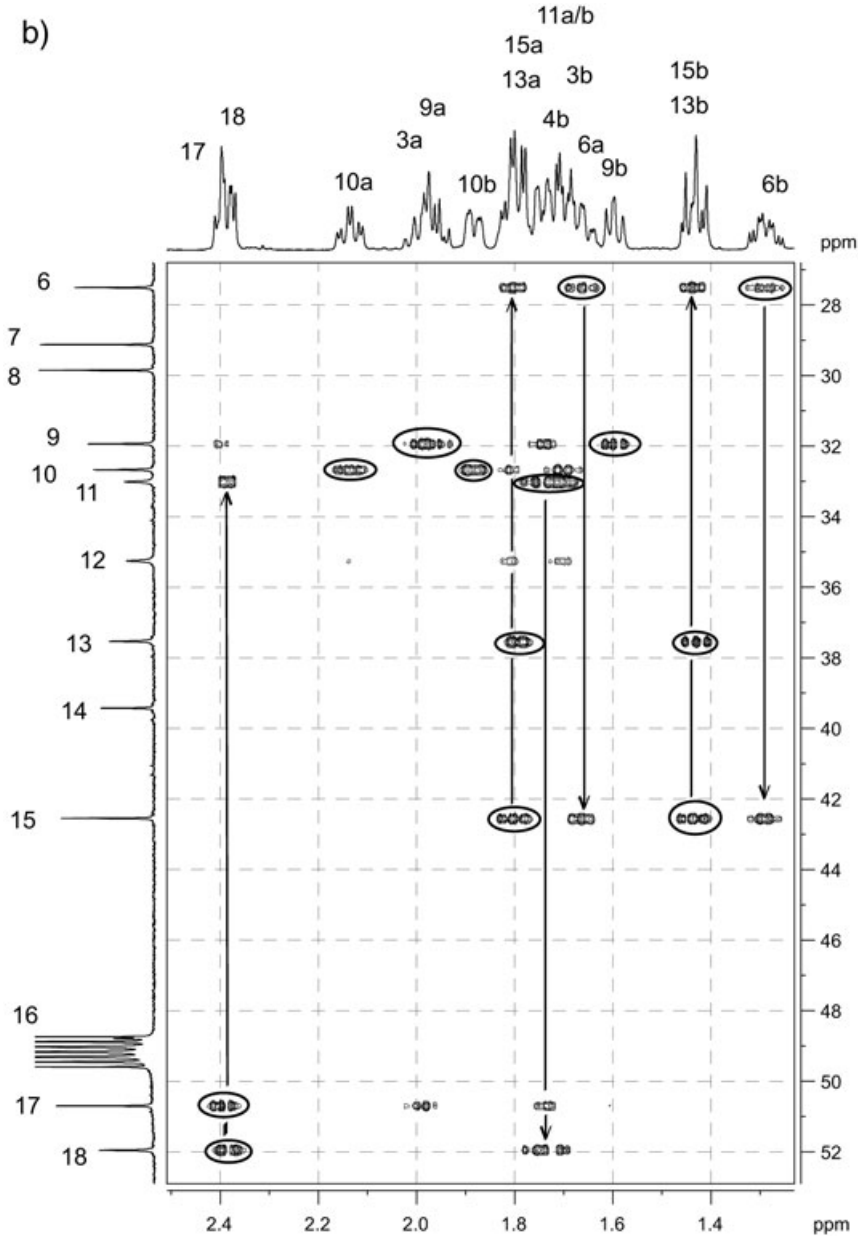

Fig. 3 (cont.)

type of NOE is observed, and, although distances in a *cis* and in a *trans* arrangement are clearly different, there are various reasons why the NOE intensities do not match the expected value (quenching of the NOE pathways by relaxation sinks, line-broadening, *etc.*). For six-membered rings, we, therefore, encourage the use of 1,3-diaxial NOEs

wherever possible. To clarify this point, typical values of distances between vicinal H-atoms in six-membered rings, assuming a chair-like conformation (which may not always be the case!), are displayed in *Fig. 4*.

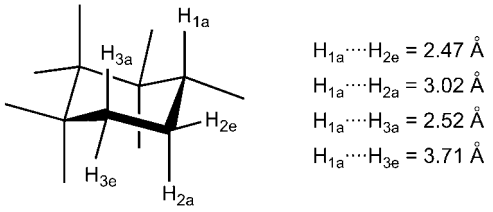

Fig. 4. *Selected interatomic H ··· H distances in a six-membered ring in chair conformation*. Not all H,H pairs are suited equally well for NOE considerations (see text).

Distances between the axial H-atom H_{1a} and the two vicinal atoms H_{2a} and H_{2e} are clearly different, but both pairs will yield reasonably intense NOEs. In contrast, the distance between H_{1a} and H_{3a} is very different from that between H_{1a} and H_{3e}, the latter usually not giving rise to an NOE cross-peak.

We would like to present an example from our own work, which involved elucidation of the configuration of a phloroglucinol derivative. A sketch of the molecule is presented in *Fig. 5*. Therein, two five-membered rings are connected to each other, one of which is again fused to a six-membered ring, giving rise to a 6*H*-3a,7-methanoazulene skeleton. Whereas the five- and six-membered-ring attachment is constrained by the bridge to be *cis*, the two five-membered rings may be attached either in a *cis* or *trans* fashion, and the relative configuration at C(2) had to be determined additionally. Building up the molecule in 3D can be done with many graphics programs. We very much recommend performing a short energy minimization using a force-field appropriate for small organic molecules (*e.g.*, MM2 [39]) to ensure that the resulting conformation is energetically reasonable. At these low levels of computation and in the absence of solvent, the resulting conformations are not expected to very closely match reality, but rather serve to provide a rough estimate of relevant distances. Distances between H-atoms that are *not* connected through rotatable bonds are still sufficiently accurate. In case a single rotatable bond is involved, measurements of distances for rotamers in 10° steps will provide the range of distances. When more than one rotatable bond is involved, distances tend to be too imprecise to be useful. In *Fig. 5*, the molecule was built once *cis*- and once *trans*-fused with respect to the C(3a)–C(8a) bond. NOEs that were useful to distinguish the two stereoisomers are marked in the models.

NMR Characteristics of Classes of Natural Products. – In the following, characteristic spectral features of some important classes of natural products will be briefly described. The probably most-easily accessible parameter is the chemical-shift dispersion. Some compound classes such as steroids, peptides, or carbohydrates can often be recognized from their 1D-^{1}H-NMR spectra. We would like to state that it is useful to keep in mind which solvents were used during the purification steps. In our experience, researchers often spend considerable time trying to assign solvent signals. *Gottlieb et al.* [40] have published a very useful compilation of chemical shifts of

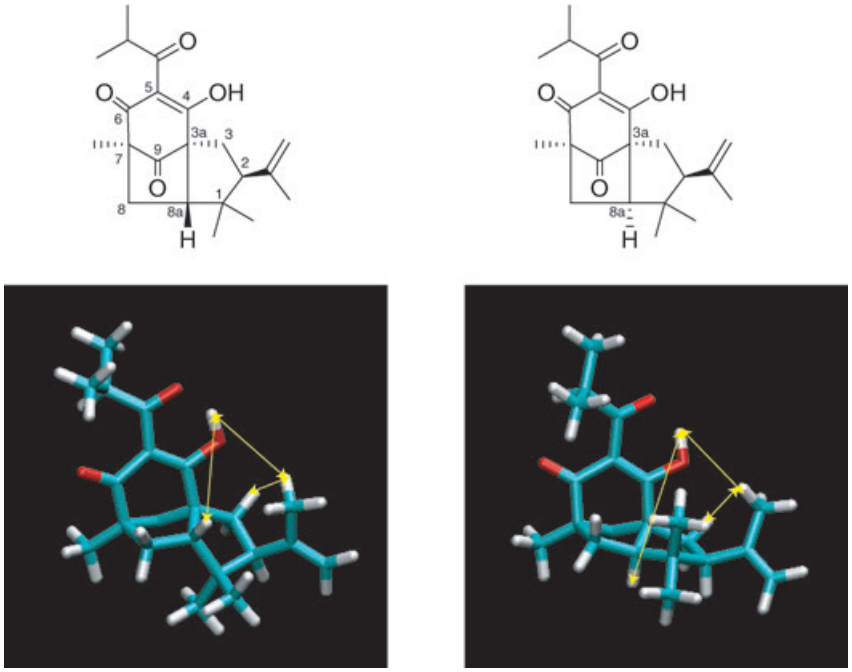

Fig. 5. *Structures of two phloroglucinol-derived isomers with either* cis- *or* trans-*fused five-membered rings* (right *vs.* left). Pertinent NOEs for structure discrimination are marked with arrows.

solvents present as trace impurities, which may help to immediately recognize such contaminations.

In *Fig. 6*, the 1D-^{1}H-NMR spectra of representative compounds, plotted from 0 to 10 ppm[3]), are shown. The representatives chosen are not extensively functionalized, and signal dispersion may actually be much larger if this is the case.

Fig. 7 presents a graphical overview of the ^{13}C-NMR chemical-shift ranges typically observed for members of the typical natural-product classes. Although compounds are generally identified from full interpretation of 2D spectra, the 1D spectra still give very useful information and should be carefully inspected. The number of ^{13}C signals may help to identify certain classes, *e.g.*, terpenes, or helps to recognize symmetry in molecules. Other features like the presence of double/triple bonds, aromatic systems, or C=O groups can also be identified immediately. The ratio of aliphatic-to-aromatic C-atoms helps to identify/exclude some compound classes. ^{13}C-NMR Chemical-shift information is of course very helpful since it allows to search in chemical-shift databases. In addition, ^{13}C-NMR chemical shifts tend to be better reproducible and are less influenced by solvent, temperature, or pH. ^{1}H-NMR Spectra reveal the presence of certain functional groups, but also acidic H-atoms such as in OH or NH. Thus, when *many* signals disappear upon adding a drop of D_2O, this may be a hint that the substance under study is a carbohydrate or a peptide.

---

[3]) Please note that certain signals often occur outside this region.

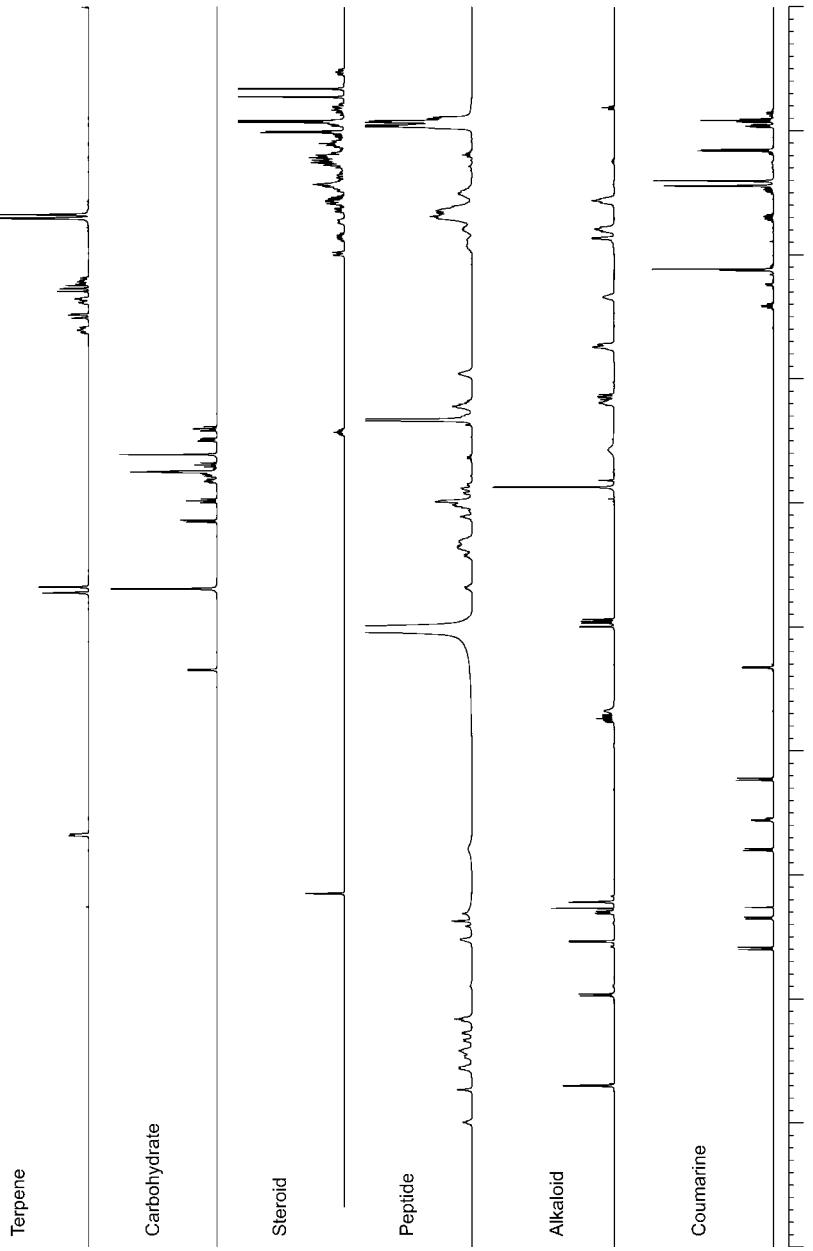

Fig. 6. *600-MHz ^{1}H-NMR Spectra of typical representatives of various classes of natural products*. From bottom to top: a *coumarine* (visnadine; in $CDCl_3$); an *alkaloid* (chinine; in $CDCl_3$); an *undecapeptide* (SGGLRLHLGLS; in 90% H_2O/D_2O); a *steroid* (5*α*-cholestan-3-ol; in (D_6)benzene); a *carbohydrate* (saccharose; in D_2O); and a *terpene* (carvone; in $CDCl_3$).

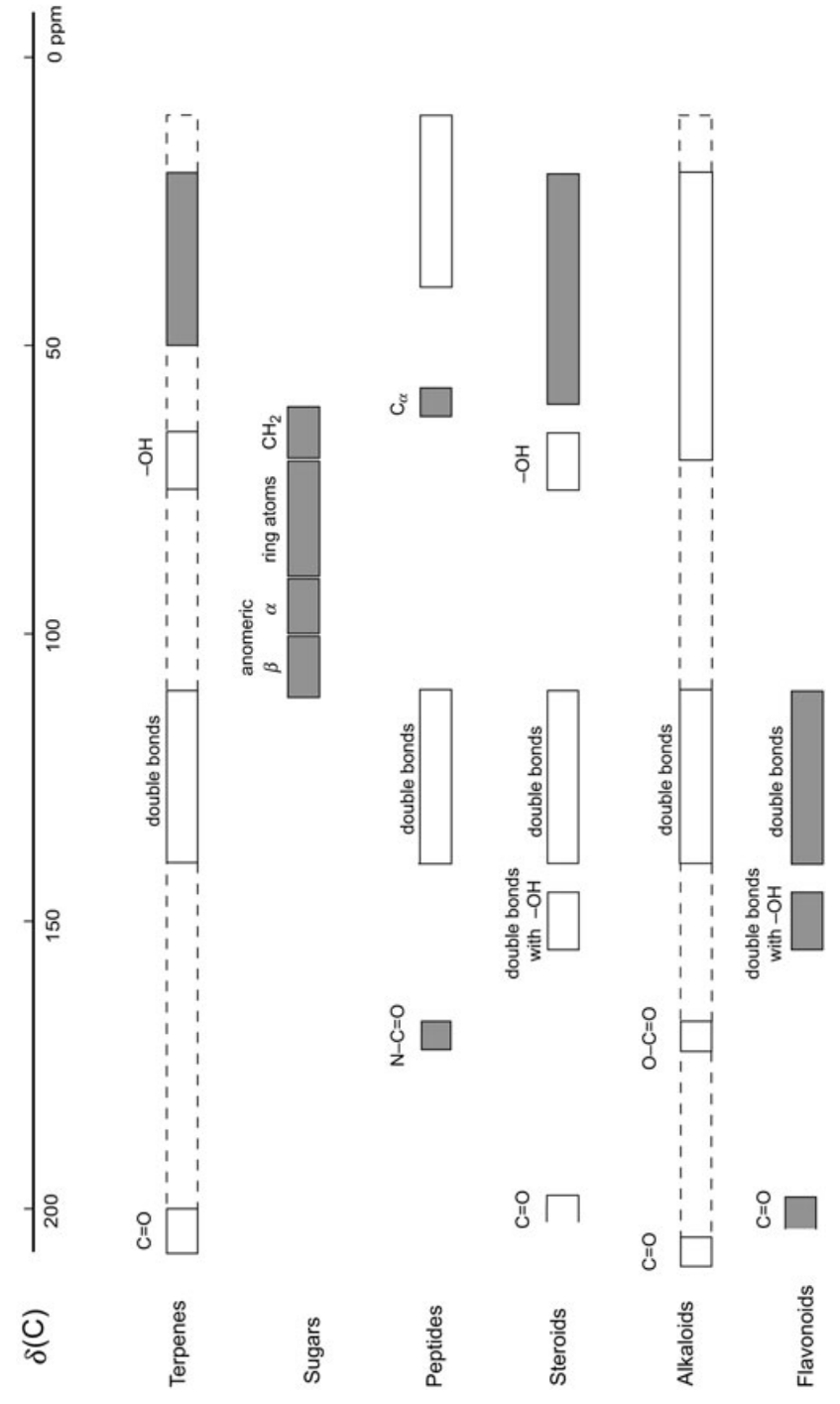

Fig. 7. *Typical ^{13}C-NMR chemical-shift ranges for selected classes of natural products.* Regions in which signals are *always* observed are indicated by filled bars, often encountered additional signal regions are represented by empty bars.

Strategies for Structure Determination. – In this review, we promote a fragment-assembly approach. Therein, short spin systems, called *fragments*, are identified from the DQF-COSY or HSQC-TOCSY spectra. These fragments are subsequently joined to each other by means of NOE- or HMBC-type information. Careful inspection of the 1D ^{1}H-NMR and, if available, ^{13}C-NMR spectra will reveal whether a strategy based on tracing along the H,H coupling network (based on DQF-COSY, TOCSY, or HSQC-TOCSY data) will be successful, or whether proton densities are so low that HMBC/INADEQUATE experiments are required to establish connectivities. It is very important to exclusively use correlations observed in the spectra and not bias the interpretation from chemical knowledge or intuition. However, once it has been recognized to which class of natural products the substance belongs, it is absolutely reasonable to adjust the strategy. Still, this approach requires no assumptions on the covalent structure.

Once it has become clear that the compound is, *e.g.*, a steroid, the skeleton can be drawn immediately. Inspection of the 1D spectrum will reveal whether ring *A* is aromatic, the degree of functionalization (in particular at C(17)), and whether the molecule contains the angular Me(18) and Me(19) groups. Again, short stretches may be recognized from the COSY, or better, from the HSQC-TOCSY spectra. However, especially when the steroid is not excessively derivatized, spin systems may be quite long, and TOCSY spectra tend to not provide much insight.

The most-powerful entry to spectral assignment of steroids is definitely *via* HMBC correlations from the angular Me groups (*singlets*), as shown in *Fig. 8*. Each Me group typically displays four rather strong correlations; these couplings are more or less conformation-independent and usually well visible. At least one of the correlations will involve a quaternary C-atom (the one to which the Me group is attached to). With the help of these and the fragments identified from the COSY/HSQC-TOCSY spectra, it is often possible to wrap up the steroid skeleton and to identify the functional groups attached to it. Rings *A* and *B* can be fused in *cis* or *trans* fashion, as is the case for rings *C* and *D*, whereas rings *B* and *C* are always fused in *trans* mode. A few key NOEs will help to quickly establish the configurations at the ring junctions (see *Fig. 8*). Please also see the excellent review by *Croasmun* and *Carlson* about the NMR analysis of steroids [41].

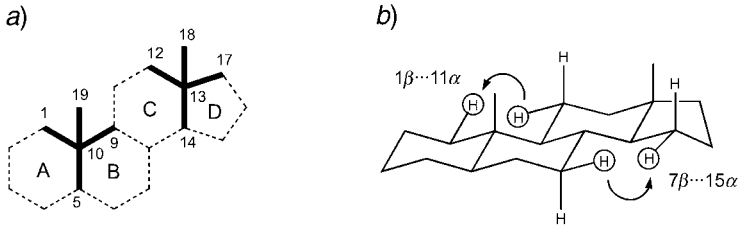

Fig. 8. a) *Useful HMBC correlations involving the angular Me groups of steroids for establishing the basic C-skeleton.* b) *Useful NOEs to elucidate the configuration at the fusion sites of rings* A/B *and* C/D*, resp.*

The presence of carbohydrates may also be immediately recognized from 1D-^{1}H- and -^{13}C-NMR spectra. Excellent reviews for carbohydrate NMR analysis have been published [42][43]. We will, thus, only briefly summarize the most-important features.

Unfortunately, carbohydrate spectra can be rather nasty due to the often-encountered presence of conformational exchange leading to excessive line broadening. Another problem is the inherent low signal dispersion. Best separation is usually found for the anomeric H-atoms. Extraction of strips along the frequencies of these signals in the TOCSY will help to establish which of the anomeric H-atoms belong to which ring system. However, especially in furanose systems, vicinal couplings tend to be rather small and can easily be smaller than the line width, so that correlations are missing in the spectra. In such cases, there is no alternative to the (careful!) use of NOEs to establish neighboring correlations. The configuration at the anomeric center may be identified from the chemical shift of the anomeric H-atom or from its vicinal coupling. Linkages between the monosaccharide units can be established by key NOESY or HMBC correlations. The exact chemical nature of the monosaccharide units requires identification of configuration at all C-atoms (axial or equatorial OH groups?). The strategy used for carbohydrates is summarized in *Fig. 9*.

At this point, it should be stressed again that the use of 1,3 NOEs to detect axial H-atoms is much preferable to 1,2 NOEs. In the case of pyranoses, the best approach is to use vicinal scalar couplings, which are large for diaxial arrangements, but much smaller for axial/equatorial or diequatorial arrangements. Because in most of the cases it is impossible to extract the couplings from the 1D spectra due to resonance overlap, this information is more easily derived from the *multiplet* patterns in the COSY spectra. Since these will be tremendously simplified when OH H-atoms (and hence their couplings) are absent from the spectra, and considering that stereochemical information may also be inferred from the position of the corresponding C-bound H-atoms, protic deuterated solvents such as CD_3OD or D_2O are recommended. Typical (simulated) patterns of COSY cross-peaks are displayed in *Fig. 10*.

The H−C(3)/H−C(2) cross-peaks of β-mannose display along F2 (the horizontal axis) the presence of a small active and a large passive coupling (identified by anti-phase or in-phase splitting, respectively), whereas, for α-glucose, two large couplings are observed (note that, in this case, cancellation of *multiplet* components has occurred!). The latter cross-peaks are similar to the corresponding ones in β-glucose, which, however, can be easily distinguished by comparison of the H−C(2)/H−C(1) cross-peaks. Note that no extraction of exact coupling constants from the cross-peaks is necessary; recognition of the overall appearance of the peak is usually sufficient.

The presence of peptides may also be easily recognized from the 1D-^{1}H-NMR spectrum. A larger number of acidic H-atoms, whose resonances disappear upon addition of D_2O, are observed low-field of 7 ppm. Because the spin systems of many amino acids look very similar, identification of the primary structure (the amino acid sequence) by means of NMR is very difficult, and chemical methods such as *Edman* degradation or sequencing by mass spectrometry are much preferable. However, when nonnatural amino acids are part of the sequence, the above-mentioned methods (at least the chemical ones) may not work. In those cases, full characterization by NMR certainly requires the use of ^{13}C-NMR chemical-shift information. This approach differs from the standard procedure of sequential resonance assignment developed by *Wüthrich* and co-workers [44], which is usually employed to assign peptides of known sequences.

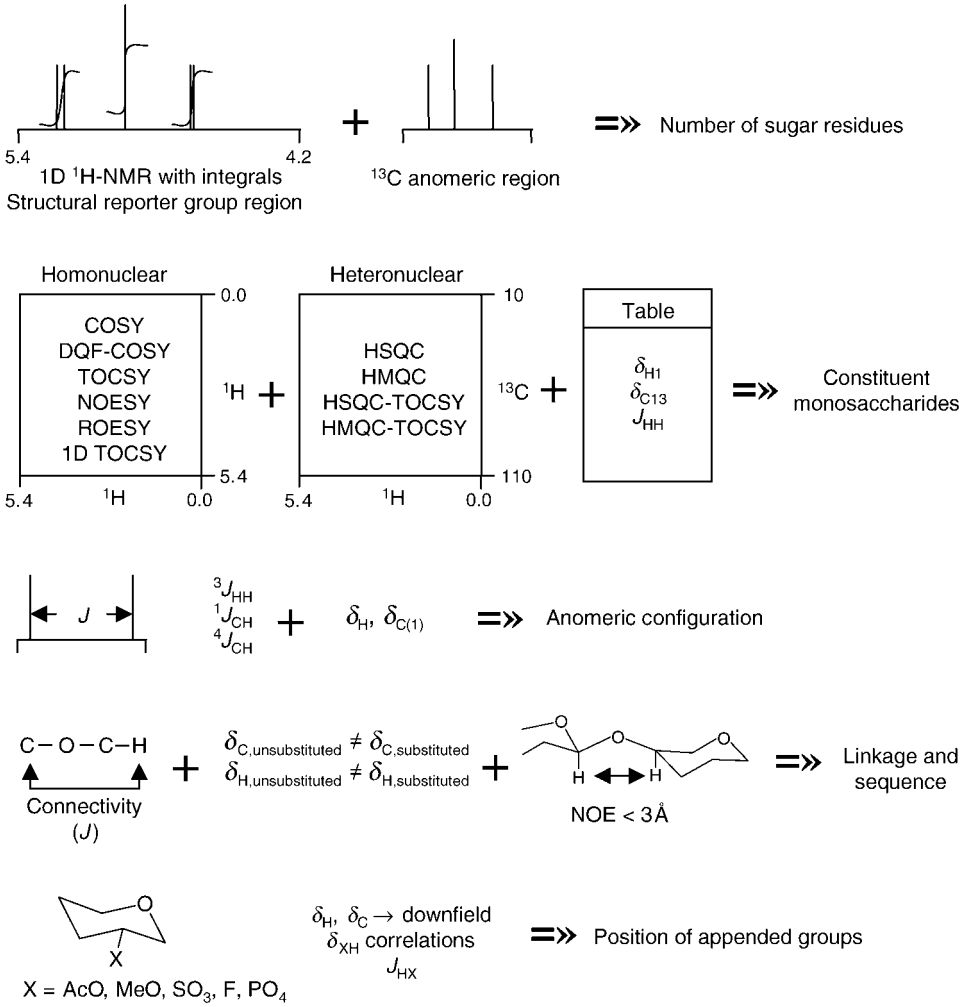

Fig. 9. *Strategy for the structure assignment of carbohydrates* (reproduced with kind permission from *Duus et al.* [42]).

Assignment and identification of peptides usually starts out with recognition of the spin systems in TOCSY spectra (*Fig. 11*). In most cases, the smallest resonance overlap is found in the region of the amide H-atoms. Amino acid side chains form separate spin systems, and no experiment that relies on coherence transfer *via* scalar H,H couplings leads to correlations between H-atoms of different residues. However, side chains may form two different spin systems, *e.g.*, for the aromatic residues. Spin systems, as recognized in the $H_N/H_{aliphatic}$ region of the TOCSY spectra, can be sorted according to certain criteria (length of spin systems, occurrence of Me signals, chemical shifts, *etc.*).

A schematic example is show in *Fig. 11,b*. Therein, typical appearances of short spin systems are sketched such as residues Cys, Trp, Phe, His (a); Val (b); Ser (c) (note that

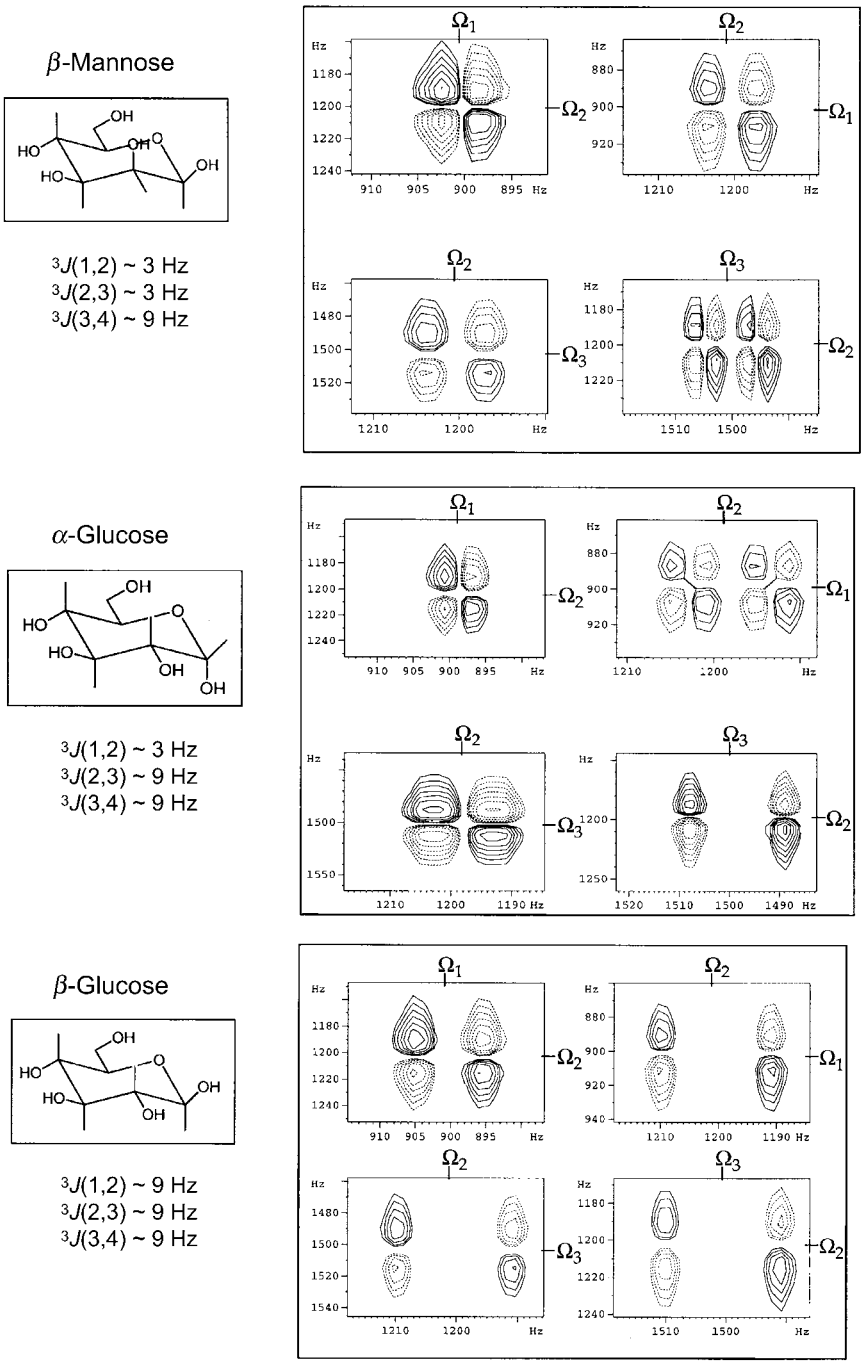

Fig. 10. *Simulated cross-peak patterns of β-mannose and α- and β-glucose in a protic, fully deuterated solvent.* Scalar couplings used for the simulation have been appended.

for serine, the β-H-atoms are shifted into the $H_{C\alpha}$ region due to the presence of the OH group); and Arg (d). Thereafter, the sequential order of spin systems is established based on NOE or HMBC information. The resulting information may be '*a Leu/Ile residue is followed by a short side-chain, followed by an Arg/Lys residue*'. Once the stretches have a certain length, the information may be unambiguously matched onto the sequence. Sequential information (information of H-atoms from residues next to each other in the sequence) may be extracted from $H_\alpha(i)$,$H_N(i+1)$ correlations, which are strong in extended parts of the polypeptide chain, or from $H_N(i)$,$H_N(i+1)$ correlations, as observed in helically folded segments. Typical values of these distances are indicated in *Fig. 11,c*.

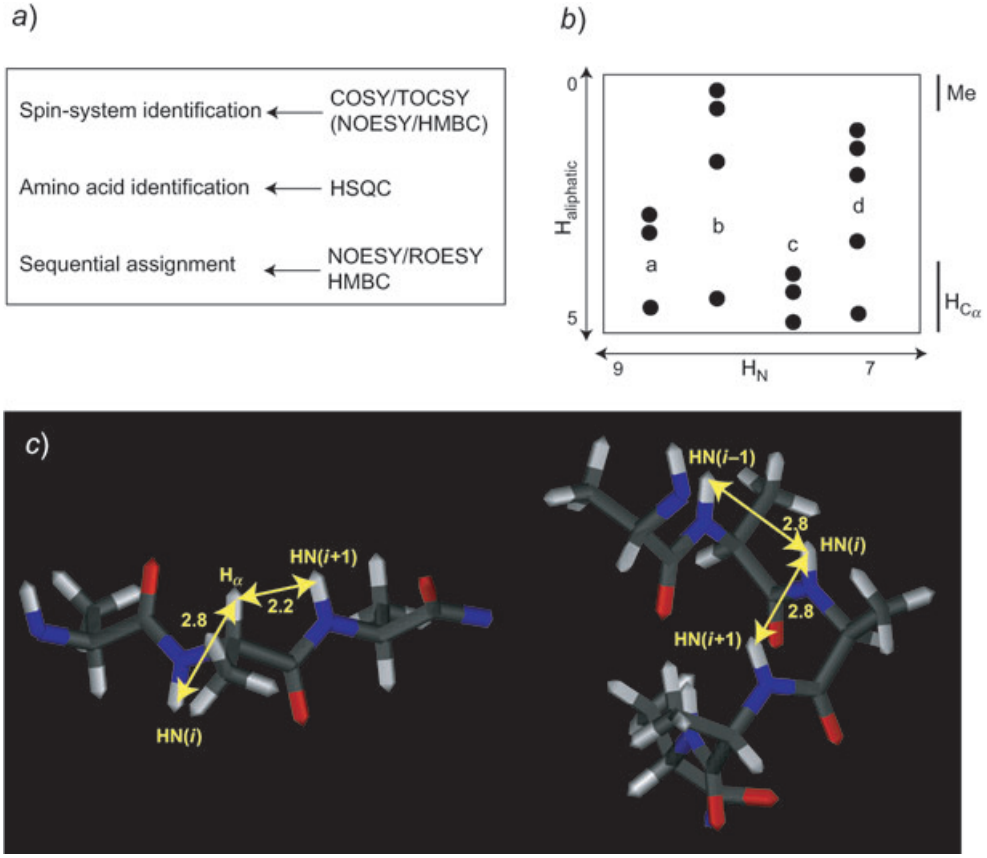

Fig. 11. a) *Strategy used for assignment of peptides of unknown sequence.* b) *Schematic presentation of spin systems as they appear in TOCSY spectra* (see text). c) *Typical distances used to identify extended* β*-sheets* (left) *or* α*-helical segments* (right).

An alternative are HMBC spectra involving correlations to a common backbone C=O resonance. Once the sequential order of the spin systems has been established, side-chains may be fully assigned by means of a combination of COSY and TOCSY spectra. If the amino acid sequence has not been established prior to the NMR studies,

HSQC/HMBC experiments are required to verify the structure from the ^{13}C-NMR chemical shifts, which will also help to better recognize the different amino acids. Such a strategy, of course, requires more material, but the HMBC correlations to the amide C=O groups may establish sequential correlations less prone to false assignments (in contrast to the use of NOEs, which may also be found across strands in β-sheets and, therefore, between residues far apart in the sequence). For a more-detailed description of the assignment methods for peptides, but also for aspects of structure determination from NMR data, see the monograph of *Wüthrich* [44], or the articles from *Williamson* [45] and *Redfield* [46].

Due to their chemical diversity, no particular strategy can be recommended for terpenes and alkaloids. Since there is also no common C-skeleton, it is very important to work with the fragment-assembly approach, and use as little assumptions as possible, or better no assumptions at all!

A Case Study: Identification of Taxol based on 2D-NMR Experiments. – *Fig. 12* displays the 1D-^{1}H- and -^{13}C-NMR spectra of taxol. The ^{1}H-NMR spectrum shows very good signal dispersion. Signals are equally distributed over the region between 1 and 8.2 ppm. However, from this spectrum alone, it is impossible to deduce the class of natural product, although it is clear that the compound is not a carbohydrate, a steroid, or a peptide. The compound to be identified contains a larger number of *singlet* Me groups and, probably, an aromatic functionality. The ^{13}C-NMR spectrum displays 41 lines (excluding solvent lines). We prefer to number signals according to increasing carbon frequencies. Following this convention C(22) to C(35) belong to aromatic or other unsaturated systems. C(36) to C(40) belong to ester/amide C=O groups, and C(41) belongs to a ketone. C(22), C(23), and C(25)–C(28) display twice the signal intensity and may, therefore, encode for two symmetric C-atoms each.

By using the [^{13}C,^{1}H]-HSQC spectrum, C-atom numbering is transferred to the ^{1}H-NMR spectrum. Hence, H(16) (*i.e.*, H–C(16)) is directly bonded to C(16). This procedure reveals that protons A–D are not C-bound. Luckily, the taxol signals are well separated and, therefore, with the help of the integrals of the ^{1}H-NMR spectrum and HSQC information, the following peak assignment may be put together:

1	CH_3	13	CH	25	2 × CH	36	C (–COO– or –CON–)
2	CH_3	14	CH	26	2 × CH	37	C (–COO– or –CON–)
3	CH_3	15	CH	27	2 × CH	38	C (–COO– or –CON–)
4	CH_3	16	CH	28	2 × CH	39	C (–COO– or –CON–)
5	CH_3	17	CH	29	C	40	C (–COO– or –CON–)
6	CH_3	18	CH_2	30	CH	41	C=O (ketone)
7	CH_2	19	C	31	CH		
8	CH_2	20	C	32	C		
9	C	21	CH	33	C	A	NH or OH
10	CH	22	2 × CH	34	C	B	NH or OH
11	CH	23	2 × CH	35	C	C	NH or OH
12	C	24	CH			D	NH or OH

From the DQF-COSY data fragments **a**–**h** may then be assembled. This step is rather straightforward, because signal dispersion in taxol is spectacular. In other cases,

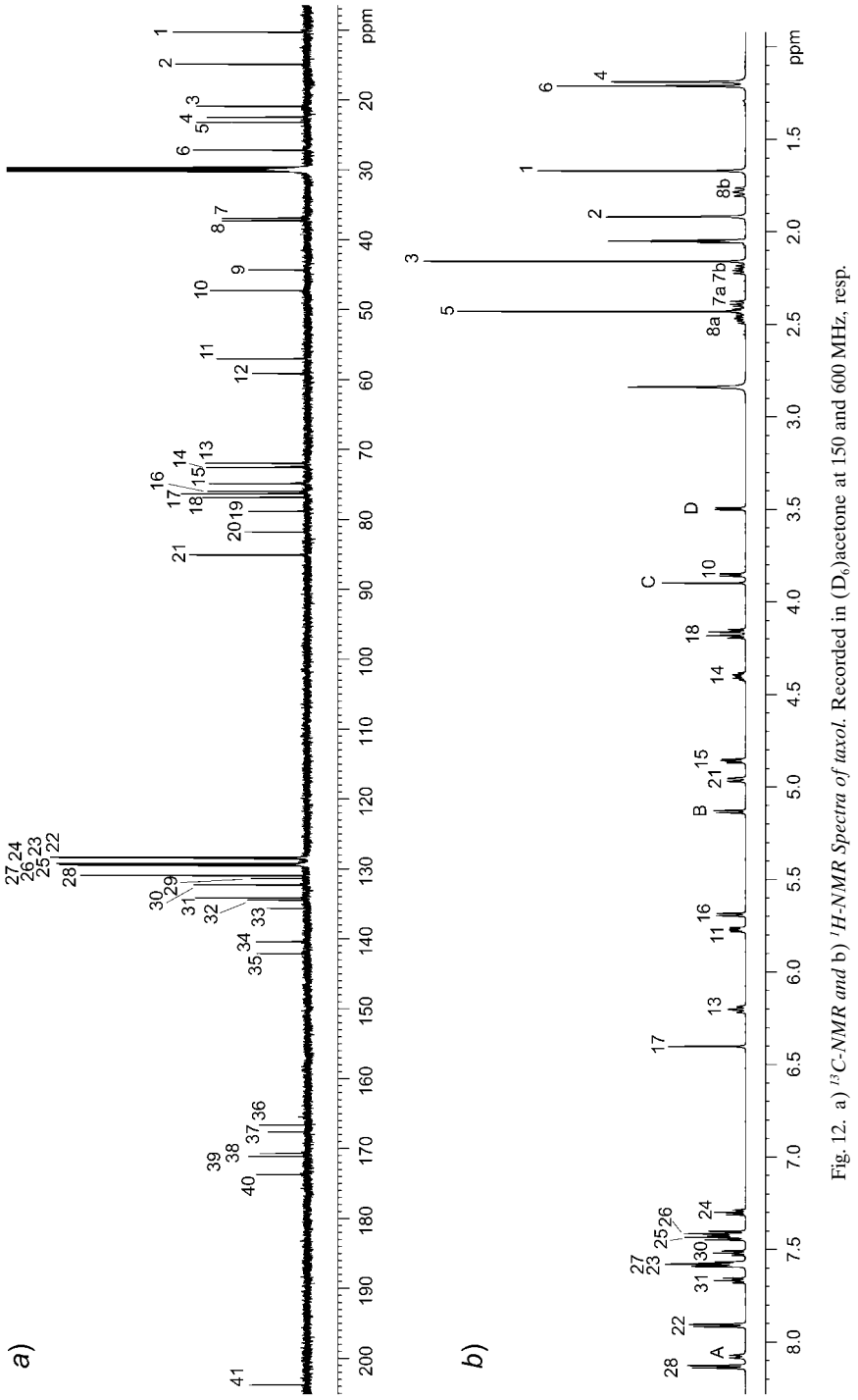

Fig. 12. a) *^{13}C-NMR and* b) *^{1}H-NMR Spectra of taxol.* Recorded in (D_6)acetone at 150 and 600 MHz, resp.

HSQC-TOCSY data may have to be used to a larger extent to facilitate assignment in crowded regions. A crucial point at this stage is to *not* make any assumptions of how these fragments may be linked (please forget your chemical intuition at this stage!).

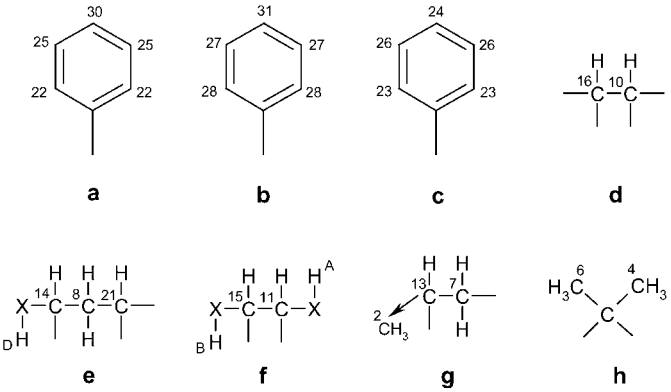

The next and (in this case) rather time-consuming step is to link the fragments **a**–**h** together. This may be done by means of NOEs or H,C long-range couplings derived from HMBC spectra. In this example, we will mainly use HMBC correlations for this purpose.

The couplings H(27) → C(36),(28),(*29*)[4]), H(25) → C(*33*),(25),(22/23), and H(26) → C(*34*),(24),(26) identify the quaternary aromatic C-atoms and their neighbors. The HMBC connectivity C(36) → H(*28*),(27),(*16*) establishes the linkage to the next moiety, resulting in fragment **I**. Similarly, H(22) → C(*37*),(22),(30), C(37) → H(*22*),(*A*),(*11*), and H(23) → C(24),(23),(*11*) link the three fragments **c**, **f,** and **a** to yield fragment **II**. The latter can be expanded by using the HMBC correlations H(B) → C(*40*),(15),(11) and C(40) → H(13),(*11*),(B) to connect fragment **g** to fragment **II** to yield fragment **III**. We now turn our attention to fragment **e**. The H(D) → C(*12*),(8),(14) correlations establish the C(12)–C(14) linkage, and the H(8b) → C(*20*),(12),(14),(21) and H(8a) → C(*20*),(14),(21) correlations indicate a C(20)–C(21) bond. Moreover, H(14) → C(*1*),C(8),(*10*) and H(1) → C(*41*),(10),(12),(14) suggest C(12)–C(10) and C(12)–C(41) linkages, respectively, which results in fragment **IV**. Since C(10) is also part of fragment **I**, fragments **I** and **IV** can be connected to yield fragment **V**.

The H(10) → C(*20*),(41),(14),(16),(18),(*19*),(12) correlations indicate that C(20) is close to C(10), and since H(10) appears as a *doublet* and, hence, the additional connectivity should be a quaternary C-atom, this is only compatible with formation of a six-membered ring by direct C(10)–C(20) linkage. The H(18) → C(*20*),(21),(*10*) HMBC peaks show that C(18) is next to C(20). We can expand this fragment by using correlations from H(16) → C(*7*),(36),(19),(10),(12) to join fragment **III** to it, resulting in fragment **VI**.

H(C) is connected to a heteroatom (H(C) → C(*19*),(7),(9),(16)), and the chemical shift of C(19) indicates that this is also true for C(19), resulting in H(C)–X–C(19).

---

[4]) *Important* correlations (position numbers) are printed in italics.

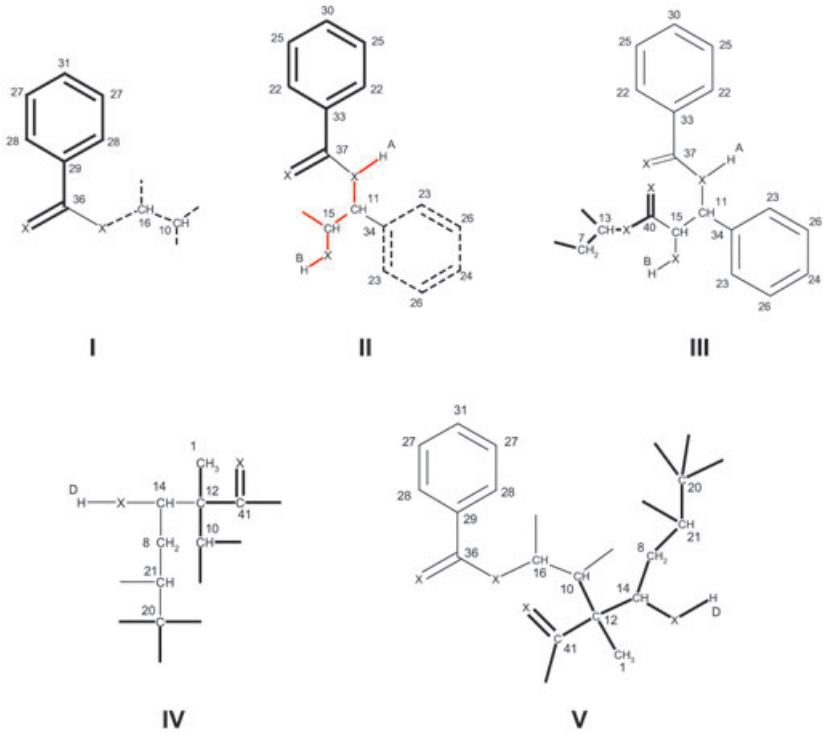

I II III IV V

The HMBC peaks C(9) → H(*7a*),(*16*),(17),(C),(2),(6),(4) establishes C(9)–C(19), and H(6) → C(4),(9),(13),(*32*),(*19*) and H(4) → C(6),(9),(*32*),(*19*) show that both C(6) and C(4) are bonded to C(9), which, in turn, is connected to C(32). The chemical shift of C(32) encodes for an sp^2 C-atom, and C(35) is the only other C-atom in that range. With C(32) → H(*17*),(13),(2),(6),(4) and C(35) → H(17),(13),(*7a*),(2), the ring closure between C(35) and C(13) is established. C(9) → H(*17*),(16),(C),(7a),(6),(4) and H(2) → C(*13*),(*32*),(35) finally define the substituents at the double bond, resulting in fragment **VII**.

Little remains to be done now! The atoms C(3), C(5), C(38), and C(39) have not been built into the structure. C(38) belongs to an ester/amide C=O group, and H(3) → C(*38*),(*17*), H(17) → C(*38*),(*41*),(32),(35),(14),(9),(12) and H(5) → C(*39*) establish the ring closure between C(41) and C(17) and the fragments **i** and **k**, respectively.

Finally, we need to establish the correct heteroatoms and fuse fragments **i** and **k** to the rest. The chemical shifts of C(13), C(17), and C(16) indicate that the neighboring C=O functions are esters. The fact that H(A) is bonded to the heteroatom establishes the amide functionality at C(37). The chemical shifts of C(18) and C(21) indicate that these atoms are bonded to an O-atom. The fact that they are bonded to the same O-atom, thereby forming the four-membered ring is not clear yet, and can only be deduced from additional mass spectral data (correct formula and molecular weight). The C(21) → H(18) HMBC peak is, unfortunately, not helpful in that respect. The chemical shift of C(20) indicates that this atom is bonded to an O-atom, and we have no

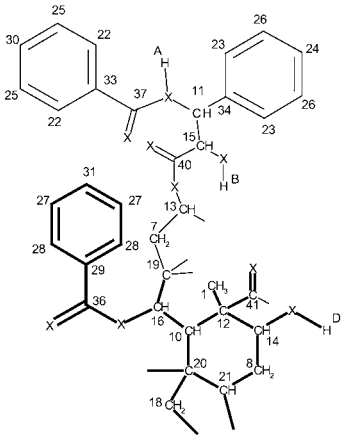

VI

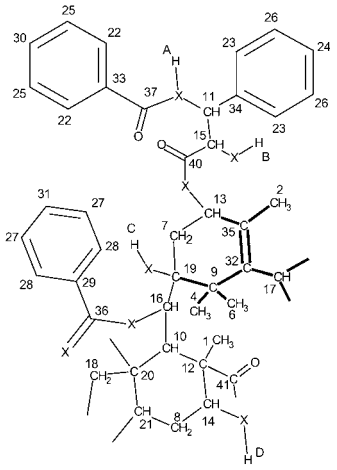

VII

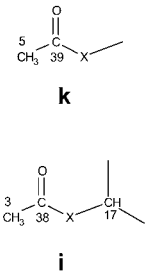

k

i

other possibility than to fuse fragment **k** to C(20). Unfortunately, we do not see any HMBC correlations for that connectivity. Finally, we end up with the correct structure of taxol (**1**). Please note that we have not made any assumption on the covalent structure nor did we use chemical intuition to establish the structure!

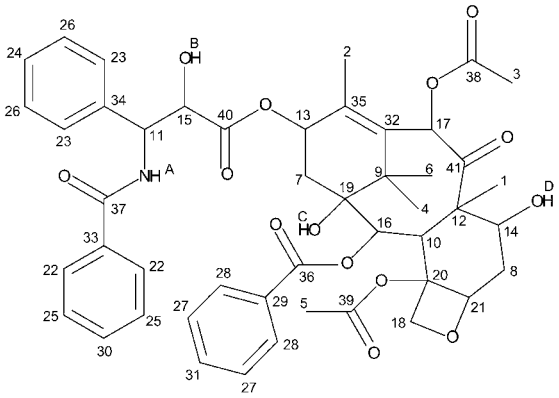

Taxol (**1**)

An even more-formidable task is the determination of the correct configuration! First of all, NMR is only capable of establishing *relative* configurations, and only in rare cases can the absolute configuration be worked out (see, *e.g.*, the method of *Mosher* for the determination of the absolute configuration of alcohols [47]). In the case of taxol, the configuration of the OH group at (according to our numbering) C(15) cannot be determined due to the conformationally rather flexible structure in this part of the molecule. The situation is clearly much better for the stereogenic centers at the fused rings. We have built a 3D model of taxol in three different configurations (*Fig. 13*).

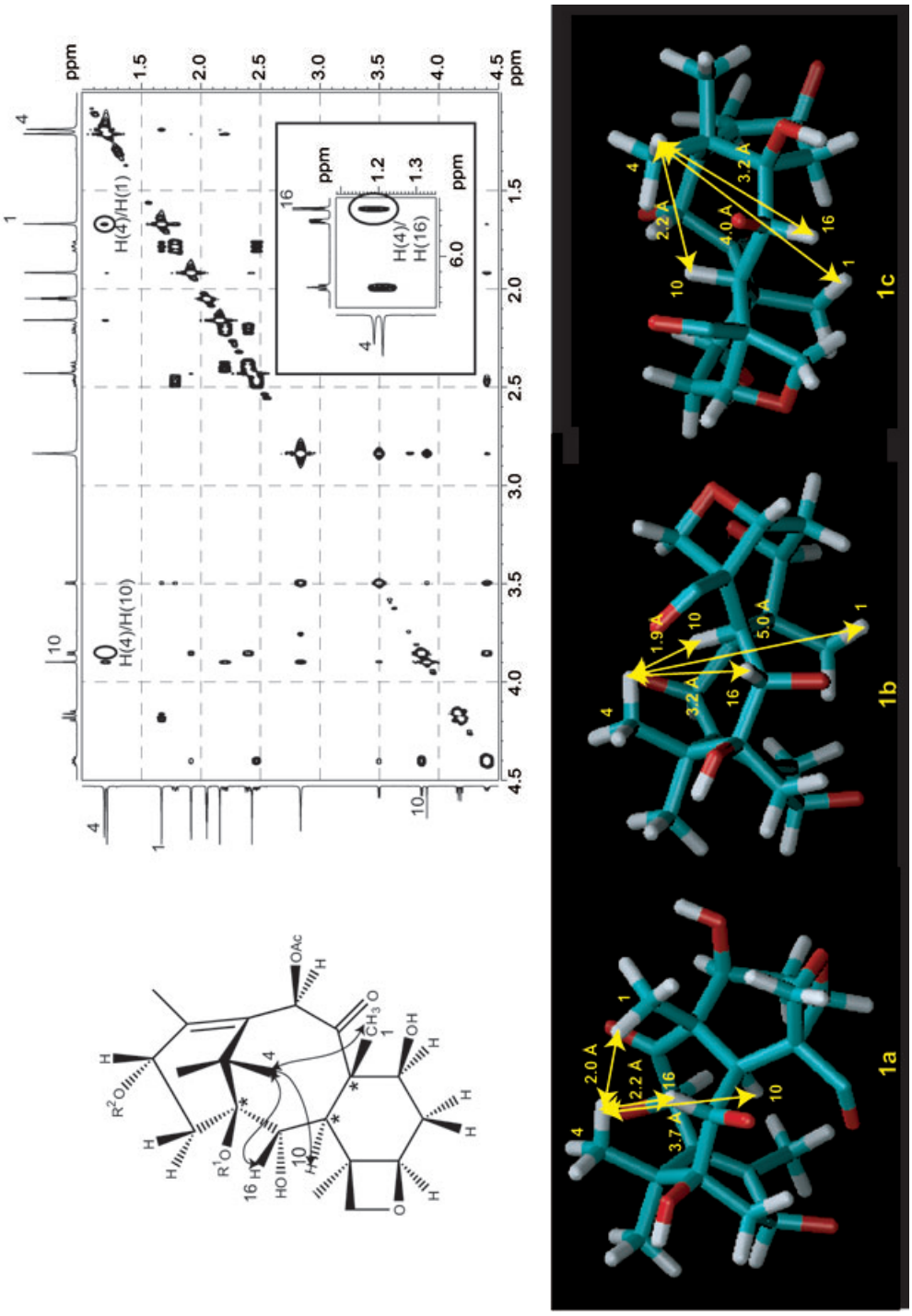

Fig. 13. *Computer-generated fragments of taxol with 'correct'* (**1a**) *and 'wrong'* (**1b** and **1c**) *configurations* (see text). The indicated intramolecular distances were derived from energy-minimized models. Also shown is an expansion of the 450-ms 600 MHz NOESY spectrum of taxol (**1a**), highlighting the presence or absence of NOE cross-peaks relevant to discriminate the three stereoisomers.

Model **1a** represents the correct stereoisomer. In model **1b**, the configurations at C(12) and C(10) are inverted, and in isomer **1c**, the configuration at C(19) is inverted. Clearly, the distance between the Me(4) H-atoms and the H-atom at C(1) is very short (*ca.* 2 Å) and, therefore, should give rise to a strong NOE only for **1a**[5]). The same is true for the H(16)···H(4) distance, which is short (2.2 Å) compared to the corresponding distances in **1b** (3.2 Å) and **1c** (3.2 Å). A distance of *ca.* 2.0–2.5 Å usually gives rise to a strong NOE, whereas distances larger than 3.5 Å will result in weak or no NOEs. However, this also depends on the overall tumbling time of the molecule. Although we strongly encourage to make use of the presence of NOEs rather than of their absence, we notice that the H(10)···H(4) distance is 3.7 Å in **1a** *vs.* 1.9 and 2.2 Å in **1b** and **1c**, respectively, which is reflected by the *absence* of such a correlation in the NOESY spectrum.

A full discussion of the elucidation of the relative configurations at all stereogenic centers of taxol is clearly out of the scope of this short review article. Other centers may be handled in a similar way as described. However, the reader should bear in mind that computer models may be rather imprecise, heavily depending on sophistication of the computational method used. Distances, therefore, have to be treated with great caution and should be used only as approximate values. Nevertheless, we again like to emphasize that such models are certainly preferable to visual inspection of chemical drawings on paper, and also to manual model building.

We would like to thank *Martin Binder* from *Hoffmann-LaRoche* and *Simon Jurt* from the University of Zurich for careful reading of and useful comments on the manuscript.

Appendix

This section gives a short overview of the most-important 2D-NMR experiments used for the identification of natural products. The summary is, by no means, comprehensive, but presents a personal selection of frequently used experiments. The principle-transfer pathways have been sketched using a small aromatic fragment. The starting H-atom is encircled, the bonds forming the pathway are printed in bold, and the correlated partner(s) is (are) indicated by a black (filled) circle.

1. *Double-Quantum-Filtered Correlated Spectroscopy: DQF-COSY*

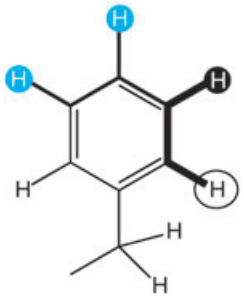

DQF-COSY is the prototype 2D-NMR experiment to identify correlations of scalar-coupled H-atoms. These are mainly vicinal; rarely, long-range couplings are also visible. Couplings should be resolved (larger than the line-width of the signals) to give rise to cross-peaks. DQF-COSY is one of the most-important experiments for establishing fragment structures.

Sensitivity: +2
Literature: [16]

---

5) The corresponding distances in **1b** and **1c** are *ca.* 4 and 5 Å, resp.

2. *Total-Correlation Spectroscopy: TOCSY*

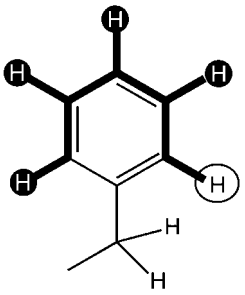

TOCSY experiments ideally yield correlations of all scalar-coupled H-atoms within a given spin system. By appropriate choice of the mixing time, either vicinal correlations (12 ms) or correlations throughout the complete spin system (*e.g.*, 80 ms) are detected. Such experiments are very important to identify compounds with separate spin systems (such as carbohydrates or peptides), as well as in case of severe resonance overlap.

Sensitivity: +3
Literature: [17][18]

3. *Two-Dimensional Nuclear*-Overhauser-*Effect Spectroscopy: NOESY*

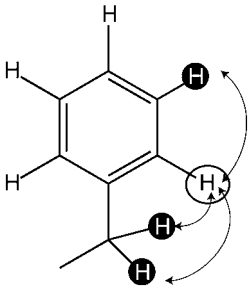

2D-NOE Experiments ideally yield correlations of dipolar-coupled H-atoms. The dipolar coupling depends on the distance (d) of spin, decreasing with $1/d^6$. Typically, only H-atoms with distances smaller than *ca.* 5 Å give rise to such correlations, independent of the number of intervening bonds. For small compounds, the mixing time should be adjusted to *T1* (the longitudinal relaxation time), but for larger molecules, a much shorter value is recommended to avoid spin diffusion. 2D-NOE is the experiment proper to establish configurations or, together with HMBC, to link fragments. For molecules in a certain size range, the NOE can actually be zero, which calls for a ROESY [19][20] experiment.

Sensitivity: +1
Literature: [21]

4. *Heteronuclear-Single- or -Multiple-Quantum-Coherence Spectroscopy: HSQC or HMQC*

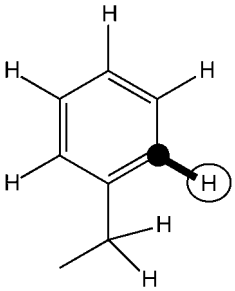

This experiment ideally identifies correlated H-atoms and the heteroatomic nuclei (mainly C-atoms) directly attached to them. It conveniently allows transferring H-atom assignments to the C-skeleton, which helps one to exploit the usually much better signal dispersion in the ^{13}C dimension. HSQC Experiments also present a way to measure ^{13}C-NMR chemical shifts of all *protonated* C-atoms, with a sensitivity much higher than in the direct measurement. The use of ^{13}C-NMR frequencies during assignment enables one to use databases for compound identification/elucidation. The use of ^{13}C-NMR chemical shifts and correlations involving C-atoms are important for compounds with few H-atoms such as, *e.g.*, flavonoids.

Sensitivity: +/–
Literature: [25] (HSQC); [26][27] (HMQC)

5. *Heteronuclear-Multiple-Bond-Correlation Spectroscopy: HMBC*

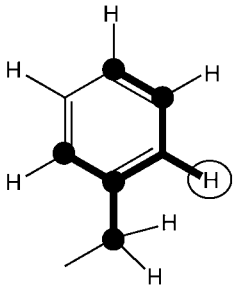

HMBC Experiments yield correlations between H- and C-atoms due to two- or three-bond scalar coupling. These couplings are usually small (< 10 Hz). Hence, these experiments are only capable of detecting correlations of reasonably sharp lines. The ^{3}J couplings follow a *Karplus*-type dependence on the dihedral angle involved. Therefore, these couplings may be small (or even zero), so that certain correlations can be missing. HMBC is important to derive chemical shifts of C-atoms lacking H-atoms (*e.g.*, C=O groups), but also to link fragments. The combination of DQF-COSY and HSQC/HMBC presents a convenient way to assign highly functionalized molecules comprising few H-atoms.

Sensitivity: – 1
Literature: [28]

6. *Combination of HSQC and TOCSY Spectroscopy*

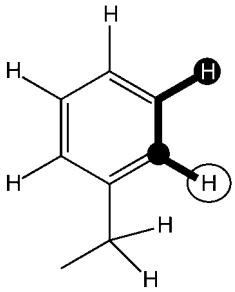

In HSQC-TOCSY experiments, the HSQC data are combined with a TOCSY transfer. Usually, the mixing time is chosen to limit transfer to *vicinal* H-atoms. HSQC-TOCSY can serve as an (although less-sensitive) alternative to DQF-COSY. It allows the assignment in fragments, in which the ^{1}H-NMR chemical-shift dispersion is poor.

Sensitivity: – 1/ – 2
Literature: [31]

7. *Incredible-Natural-Abundance-Double-Quantum-Transfer Spectroscopy: INADEQUATE*

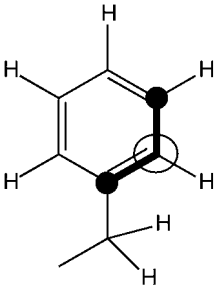

INADEQUATE is a homonuclear 2D shift-correlation experiment. It is a specially designed COSY experiment that yields ^{13}C,^{13}C correlations, efficiently suppressing the much more-abundant ^{13}C,^{12}C fragments. The bottleneck of this highly versatile experiment is its extremely low sensitivity. Large sample quantities (typically > 10 mg) are required. However, when spectra with a sufficient signal-to-noise ratio have been recorded, assignment is straightforward, even for extremely highly functionalized compounds. Recent improvements in probe sensitivity have significantly increased the usefulness of this technique.

Sensitivity: – 3
Literature: [9]

REFERENCES

[1] R. R. Ernst, W. A. Anderson, *Rev. Sci. Instr.* **1966**, *37*, 93.
[2] W. P. Aue, E. Batholdi, R. R. Ernst, *J. Chem. Phys.* **1976**, *64*, 2229.
[3] R. Freeman, G. A. Morris, *Bull. Magn. Reson.* **1979**, *1*, 5.
[4] G. E. Martin, R. C. Crouch, in 'Two-Dimensional NMR Spectroscopy: Applications for Chemists and Biochemists', Eds. R. M. K. Carlson, W. R. Croasmun, Wiley-VCH, Weinheim, 1994, p. 873.
[5] W. F. Reynolds, R. G. Enriquez, *J. Nat. Prod.* **2002**, *65*, 221.
[6] P. Styles, N. F. Soffe, C. A. Scott, D. A. Cragg, F. Row, D. J. White, P. C. White, *J. Magn. Reson.* **1984**, *60*, 397.
[7] D. J. Russell, C. E. Hadden, G. E. Martin, A. A. Gibson, A. P. Zens, J. L. Carolan, *J. Nat. Prod.* **2000**, *63*, 1047.
[8] J. Keeler, R. T. Clowes, A. L. Davis, E. D. Laue, *Methods Enzymol.* **1994**, *239*, 145.
[9] A. Bax, R. Freeman, T. A. Frenkiel, *J. Am. Chem. Soc.* **1981**, *103*, 2102; A. Bax, R. Freeman, S. P. Kempsell, *J. Am. Chem. Soc.* **1980**, *102*, 4849
[10] D. Moskau, O. Zerbe, in 'BioNMR in Drug Research', Ed. O. Zerbe, Wiley-VCH, Weinheim, 2003, p. 67.
[11] W. Wilker, D. Leibfritz, R. Kerssebaum, W. Berml, *Magn. Reson. Chem.* **1993**, *31*, 287.
[12] K. Albert, in 'NMR Spectroscopy in Drug Development and Analysis', Eds. U. Holzgrabe, K. Albert, I. Iwawer, B. Diel, Wiley-VCH, Weinheim, 1999.
[13] J. C. Lindon, J. K. Nicholson, I. D. Wilson, *Prog. Nucl. Magn. Reson. Spectrosc.* **1996**, *29*, 1.
[14] K. Albert, 'On-Line LC–NMR and Related Techniques', John Wiley & Sons, New York, 2002.
[15] M. Godejohann, A. Preiss, C. Mugge, G. Wunsch, *Anal. Chem.* **1997**, *69*, 3832.
[16] U. Piantini, O. W. Sørensen, R. R. Ernst, *J. Am. Chem. Soc.* **1982**, *104*, 6800.
[17] A. Bax, D. G. Davis, *J. Magn. Reson.* **1985**, *65*, 355.
[18] L. Braunschweiler, R. R. Ernst, *J. Magn. Reson.* **1983**, *53*, 521.
[19] D. G. Davis, A. Bax, *J. Magn. Reson.* **1985**, *64*, 533; A. Bax, D.G. Davis, *J. Magn. Reson.* **1985**, *63*, 207.
[20] A. A. Bothner-By, R. L. Stephens, J.-M. Lee, *J. Am. Chem. Soc.* **1984**, *106*, 811.
[21] S. Macura, R. R. Ernst, *Mol. Phys.* **1980**, *41*, 95.
[22] J. F. G. Vliegenthart, L. Dorland, H. van Halbeek, *Carbohydr. Chem. Biochem.* **1983**, *41*, 209.
[23] D. Neuhaus, M. Williamson, 'The Nuclear Overhauser Effect in Structural and Conformational Analysis', Wiley-VCH, Weinheim, 1989.
[24] T. L. Hwang, A. J. Shaka, *J. Am. Chem. Soc.* **1992**, *114*, 3157.
[25] G. Bodenhausen, D. J. Ruben, *Chem. Phys. Lett.* **1980**, *69*, 185.
[26] L. Müller, *J. Am. Chem. Soc.* **1979**, *101*, 4481.
[27] A. Bax, R. H. Griffey, B. L. Hawkins, *J. Magn. Reson.* **1983**, *55*, 301.
[28] A. Bax, M. Summers, *J. Am. Chem. Soc.* **1986**, *108*, 2093.
[29] M. Jaspars, *Nat. Prod. Rep.* **1999**, *16*, 241.
[30] M. E. Elyashberg, K. A. Blinov, A. J. Williams, E. R. Martirosian, S. G. Molodtsov, *J. Nat. Prod.* **2002**, *65*, 693.
[31] L. Lerner, A. Bax, *J. Magn. Reson.* **1986**, *69*, 375.
[32] B. Reif, M. Kock, R. Kerssebaum, H. Kang, W. Fenical, C. Griesinger, *J. Magn. Reson., Ser. A* **1996**, *118*, 282.
[33] A. Bax, S. Grzesiek, *Acc. Chem. Res.* **1993**, *26*, 131.
[34] H. Kessler, M. Gehrke, C. Griesinger, *Angew. Chem., Int. Ed.* **1988**, *27*, 490.
[35] R. Freeman, 'Nuclear Magnetic Resonance', 1st edn., Longman Scientific & Technical, New York, 1988.
[36] S. W. Homans, 'A Dictionary of Concepts in NMR', 1st edn., Clarendon Press, Oxford, 1989.
[37] G. E. Martin, A. S. Zektzer, 'Two-Dimensional NMR Methods for Establishing Molecular Connectivity', Wiley-VCH Publishers, New York, 1990.
[38] W. E. Hull, 'Experimental Aspects of Two-Dimensional NMR', in 'Two-Dimensional NMR Spectroscopy', 2nd edn., Eds. W. R. Croasmun, R. M. K. Carlson, VCH Publishers, New York, 1994, p. 67.
[39] N. L. Allinger, *J. Am. Chem. Soc.* **1977**, *99*, 8127.
[40] H. E. Gottlieb, V. Kotlyar, A. Nudelman, *J. Org. Chem.* **1997**, *62*, 7512.
[41] W. R. Croasmun, R. M. K. Carlson, in 'Two-Dimensional NMR Spectroscopy: Applications for Chemists and Biochemists', Eds. W. R. Croasmun, R. M. K. Carlson, Wiley-VCH, Weinheim, 1994, p. 785.

[42] J. Duus, C. H. Gotfredsen, K. Bock, *Chem. Rev.* **2000**, *100*, 4589.
[43] P. K. Agrawal, *Phytochemistry* **1992**, *31*, 3307.
[44] K. Wüthrich, 'NMR of Proteins and Nucleic Acids', J. Wiley & Sons, 1986.
[45] M. P. Williamson, *Nat. Prod. Rep.* **1993**, *10*, 207.
[46] C. Redfield, in 'NMR of Macromoleccules', Ed. G. C. K. Roberts, IRL Press, Oxford, 1993, p. 71.
[47] J. A. Dale, H. S. Mosher, *J. Am. Chem. Soc.* **1968**, *90*, 3732.

Received October 28, 2004